COSMIC MAGNETISM SCIENCE IN THE SKA1 ERA

Authors
F. Govoni, M. Johnston-Hollitt, I. Agudo, T. Akahori[1], R. Beck, A. Bonafede, T.D. Carozzi, S. Colafrancesco, L. Feretti, K. Ferrière, B.M. Gaensler, L. Harvey-Smith, M. Haverkorn, G.H. Heald, S.A. Mao, L. Rudnick, D. Schnitzeler, A. Scaife, J.M. Stil, K. Takahashi, A.R. Taylor, O. Wucknitz.

Executive Summary
The capability of the Square Kilometre Array (SKA) will already permit in its Phase-1 (SKA1) to explore Cosmic Magnetism in a variety of astrophysical sources. Wide-band spectro-polarimetry surveys at $\simeq$1 GHz, complemented by deep polarization observations at lower and higher frequencies, will be crucial to build the foundation for SKA Phase-2 (SKA2) experiments and will allow initial studies of magnetic fields in the Milky Way, in many external galaxies and clusters, and the overall magnetized intergalactic medium.

With the intent to maximize the scientific return of the science drivers discussed in this document, we underline some inputs to the SKA1 System Baseline Design, important in the Cosmic Magnetism context. The connecting point for the Cosmic Magnetism experiments presented in this document is the SKA1 extraordinary potential for high sensitivity surveys characterized by a broadband frequency coverage. Some of the following inputs have been discussed in the SKA Continuum Assessment Workshop (9-11 September 2013, SKA Office Jodrell Bank), in the SKA Engineering Meeting (7-11 October 2013, Manchester), and in the SKA Cosmic Magnetism Assessment Workshop (22-24 January 2014, SKA Office Jodrell Bank). In the following we summarize our main requirements and we give specific recommendations in Sect. 2:

• Proper information on polarization performances are missed in the Baseline Design.
• We support the possibility of having SKA1-low with a collecting area better distributed over longer baselines. This will permit not only reduction in the confusion limit, but also of the beam depolarization.
• We support the possibility of VLBI capabilities and, if feasible, high frequency coverage (up to 15−22 GHz) at least for part of the array. This is probably more easily implemented on SKA1-mid by employing Wide Band Single Pixel Feeds.
• There is an apparent similarity between SKA1-mid and SKA1-survey capabilities. We suggest to optimize some aspects of one of the two instruments for deep observations and some aspects of the other instrument for wide-field observations. A higher survey speed is recommended for the instrument dedicated to wide-field observations.
• To not limit the possibility to detect large angular scale structures, we recommend to reduce as much as possible the distance between dishes (SKA1-mid and SKA1-survey) and between the stations (SKA1-low). We also recommend SKA1-low stations no larger than $\simeq$35 m in diameter.
• It is desirable not to have gaps in frequency range between SKA1-low and SKA1-survey/SKA1-mid, even in the initial phases of the project.

1 Introduction

Much of what is known about Cosmic Magnetism comes from sensitive total intensity (Stokes I) and polarization (Stokes Q and U) radio observations. This is because the radio emission of astrophysical sources is mainly due to synchrotron radiation which is a direct probe of relativistic electrons gyrating around magnetic field lines. The observed total intensity of the synchrotron

[1]On behalf of the Japan SKA consortium cosmic magnetism (SKAJP-Magn).

emission is related to the field strength, while the fraction of polarized emission is related to the field's degree of ordering.

In addition, the observed polarization angle Ψ of a source is modified from its intrinsic value (Ψ_0) by the effect of Faraday rotation, caused by a magneto-ionic medium (e.g. interstellar, intracluster, and intergalactic medium) between the source of polarized emission and the telescope. To describe the Faraday rotation, we use the Faraday depth of a magneto-ionic medium (Burn 1966):

$$\phi(\mathbf{l})_{[rad/m^2]} = 812 \int_{L[kpc]}^{0} n_{e[cm^{-3}]}(l) B_{||[\mu G]}(l) \mathrm{d}l \tag{1}$$

where n_e is the plasma electron density, $B_{||}$ is the strength of the magnetic field component along the line of sight, and L is the path length along the line of sight.

In the simplest possible scenario in which the radio source is located in the background of the magneto-ionic medium, the Rotation Measure (RM), which correspond to the Faraday depth calculated along the entire magneto-ionic medium path, is an observational quantity given by the slope of the variation of the polarization angle with λ^2:

$$\Psi = \Psi_0 + \mathrm{RM} \times \lambda^2 = \Psi_0 + \mathrm{RM} \times \left(\frac{c}{\nu}\right)^2 . \tag{2}$$

where λ is the observation wavelength.

When the magneto-ionic medium emits a polarized radio signal, the radio emission and the Faraday rotation are mixed. In this case the polarized radiation will in general be emitted over a range of physical distances and also over a range of Faraday depths. As a consequence, the polarization angle will no longer vary linearly with λ^2 and the emission spectrum in Faraday space can be recovered using the technique of Rotation Measure Synthesis (see Sect. 1.1).

The capability of SKA1 in performing spectro-polarimetric observations with high polarization purity, angular resolution, and sensitivity, will permit exploitation of Cosmic Magnetism in a variety of astrophysical sources. An all-sky polarization survey performed with SKA1 will provide a tightly packed distribution of RM measurements in any direction, permitting a great increase of the density of known polarized background sources on the sky (see also the SKA Magnetism Key Science Project; Gaensler et al. 2004, Beck & Gaensler 2004). These data, combined with progress in numerical techniques, will permit to track the evolution of magnetic fields in the interstellar medium, in Active Galactic Nuclei, in the intracluster medium, at the boundary of galaxy clusters, in the bridges that join clusters, and in the filamentary cosmic web. In addition, the SKA1 will make it possible to investigate magnetic fields at high redshift. Studying the evolution of magnetic fields might lead to the origin of magnetism and constrain the mechanism of their maintenance and amplification. In addition, a detailed knowledge of magnetic fields play a fundamental role in constraining the evolution of galaxies and cosmic structures in the cosmological context, both observational and theoretical. Finally, the wide-frequency coverage of SKA1 will permit to accurately measure the spectrum of the radio sources. The spectral curvature contains important information about the energy losses and gains of the synchrotron-emitting electrons.

This document has been produced in the context of the SKA Cosmic Magnetism Science Working Group and its aim is to provide inputs to the SKA1 System Baseline Design (Dewdney et al. 2013), with the intent to maximize the scientific return of the instrument already in its initial phase.

In Sect. 2 we describe our most important technical requirements, as derived from the SKA1 System Baseline Design and the outputs of the 2013 SKA Engineering Meeting. In Sect. 3 we describe possible performance values achievable by spectro-polarimetric surveys performed at $\simeq$1

GHz with SKA1. Finally, in Sect. 4, we will articulate specific Cosmic Magnetism science goals in the SKA1 era. The state-of-the-art scientific cases discussed in this section will be achieved both thanks to the proposed wide-area polarization surveys at $\simeq$1 GHz as well as thanks to deep polarization observations, over the entire range of frequencies available for SKA1, on specific regions of the sky.

1.1 Rotation Measure Synthesis

Rotation Measure Synthesis Fourier-transforms the complex polarization data from a limited part of the λ^2-space into a data cube with Faraday depth (ϕ) as the third coordinate (e.g. Brentjens & de Bruyn 2005, Heald 2009, Schnitzeler et al. 2009, Pizzo et al. 2011, Macquart et al. 2012). Bell & Ensslin (2012) have shown that also the Faraday Synthesis is a promising approach in reconstructing the polarized signal.

The interpretation of the output of Rotation Measure Synthesis is not straightforward. In particular, there is not simple relation between Faraday depth and geometrical depth. The output of the Rotation Measure Synthesis is characterized by different instrumental parameters:
i) The Rotation Measure Synthesis resolution in Faraday space, which is mainly determined by the FWHM of the main lobe of the Rotation Measure Spread Function (which is approximately of Gaussian shape), is given by:

$$\delta\phi_{[rad/m^2]} \simeq \frac{2\sqrt{3}}{\Delta\lambda^2_{[m^2]}} \tag{3}$$

where $\Delta\lambda^2$ is the width of the λ^2 coverage of the observation. A large range of $\Delta\lambda^2$ increases the RM resolution. Rotation Measure Synthesis with SKA1 takes advantage of the wide $\Delta\lambda^2$ achievable at low frequencies while also covering small λ^2 where depolarization is minimal.
ii) The maximum observable Faraday depth, before bandwidth depolarization within the channel become important, is:

$$\phi_{max[rad/m^2]} \simeq \frac{\sqrt{3}}{\delta\lambda^2_{[m^2]}} \tag{4}$$

where $\delta\lambda^2$ is the spacing between adjacent λ^2 samples (channels).
iii) The maximum observable Faraday depth width of a feature which is extended in Faraday depth space, before strong internal depolarization occurs, is:

$$L_{\phi,max[rad/m^2]} \simeq \frac{\pi}{\lambda^2_{min[m^2]}} \tag{5}$$

where λ^2_{min} is the smallest value of λ^2 of the observation. This is similar to the missing-spacings (see Sect. 2.4) problem in synthesis imaging and hence may need combination of telescopes operating at low and high frequencies. There are clearly many analogies between Rotation Measure Synthesis and synthesis imaging, with the concepts of λ^2 coverage and uv-coverage, and of an Rotation Measure Spread Function and a synthesized beam.

2 SKA1 Baseline Design: the Cosmic Magnetism point of view

In the following we provide inputs to the SKA1 Baseline Design on the basis of the scientific requirements of the Cosmic Magnetism. In particular we will concentrate on the frequency range, angular resolution, field of view, largest angular size, polarization purity, and survey speed provided by SKA1-mid, SKA1-survey, and SKA1-low. Some of the following inputs have been discussed in

Table 1: Output of the Rotation Measure Synthesis for SKA1 observations.

Instrument	Frequency range* MHz	$\Delta\lambda^2$ m^2	λ^2_{min} m^2	$\delta\phi$ rad/m^2	$L_{\phi,max}$ rad/m^2
SKA1-low	50−350	35.2	0.73	0.1	4.3
SKA1-mid	350−1050 (Band1)	0.65	0.08	5.3	38.5
	950−1760 (Band2)	0.07	0.03	49.1	108.3
	1650−3050 (Band3)	0.023	0.009	148.3	325.2
SKA1-survey	350−900 (PAF Band1)	0.62	0.11	5.6	28.3
	650−1670 (PAF Band2)	0.18	0.03	19.2	97.5
SKA1	50−3050 (All Bands)	35.9	0.009	0.1	325.2

* In the SKA1-low frequency range, sometimes the Baseline Design gives 50 − 300 MHz and sometimes 50 − 350 MHz. This needs to be clarified. There is also a discrepancy regarding SKA1-survey: in Section 2.3 on Pag.16 and in Table 1 on Pag.18, it says that the proposed frequency range for SKA1-survey is 650-1670 MHz. However, in Table 15 on Pag.71, the specifications describe three PAF bands, covering 350-4000 MHz (with 650-1670 MHz corresponding only to "PAF band 2").

the SKA Continuum Assessment Workshop (9-11 September 2013, SKA Office Jodrell Bank), in the SKA Engineering Meeting (7-11 October 2013, Manchester), and in the SKA Cosmic Magnetism Assessment Workshop (22-24 January 2014, SKA Office Jodrell Bank).

2.1 Frequency range

In the Baseline Design it is stated that only a limited number of receivers will be available for SKA1. In the following we will focus on SKA1-low and on the lower frequency receivers of SKA1-mid (Band1, Band2, Band3), and SKA1-survey (PAF Band1, PAF Band2). However, observations at higher frequencies are extremely important and Cosmic Magnetism requires a wide range of frequencies with observations spanning from 50 MHz up to >3 GHz. In high frequencies observations, moderate Faraday rotation and internal depolarization are expected to have a weak effect on the observed polarization thus reflecting the intrinsic linear polarization properties of the sources.

To guide initial Cosmic Magnetism studies in the SKA1 era, the possibility to perform wide-band spectro-polarimetry surveys at ≃1 GHz (see Sect. 3), complemented by deep polarization observations at lower frequencies, and perhaps also at much higher frequencies for the needed cases, is crucial.

By fitting Eq. 2, it will be possible to measure the RM towards a large number of bright background sources (see Sect. 3.1), for which the foreground is a Faraday screen and no internal depolarization occurs. In regions, where radio emission and Faraday rotation are mixed, the Faraday rotation effect leads to a frequency-dependent depolarization (internal depolarization) of the radio signal, which increases with decreasing frequency. To avoid significant internal depolarization (e.g. Burn 1966, Tribble 1991, Arshakian & Beck 2011), the polarized signal of regions, where emission and Faraday rotation are mixed, is generally best observed at frequency of 1 GHz or greater. In particular, for sources with $|RM| > 100$ rad/m^2 (e.g. background quasars), observing frequencies ≥5 GHz are desirable to avoid strong signal depolarization. When quasars are employed as background sources, to disentangle their strong internal Faraday rotation from that in intervening sources, high frequency coverage up to ≃22 GHz (at least for part of the array) would be desirable to measure the contribution from the strong component of Faraday rotation.

The high sensitivity provided by SKA1 will make possible to observe the polarized signal in narrow frequency channels over large bandwidths, and hence to exploit the Rotation Measure synthesis at its best to recover the polarized signal affected by depolarization and/or fit depolarization models to data.

As mentioned in Sect. 1.1, the observing frequency range determines the output of the Rotation Measure Synthesis. A large λ^2 coverage is necessary to obtain a high resolution in Faraday space. In addition, it is important to mention that gaps in the frequency coverage lead to side-lobes of the Rotation Measure Spread Function.

In Table 1, we summarize the Rotation Measure Synthesis performances for SKA1-low, SKA1-survey, and SKA1-mid. The highest resolution in Faraday space ($\delta\phi$) and hence the highest precision to measure Faraday depth components is achieved with SKA1-low, while the maximum observable Faraday depth width ($L_{\phi,max}$) of a feature which is extended in Faraday depth space is provided by SKA1-mid. Although SKA1-low formally gives a much better Faraday depth resolution, internal Faraday depolarization also increases strongly with λ, so that the various frequency ranges are highly complementary for Cosmic Magnetism studies, by giving leverage on different aspects of the physics of the sources. Finally, as shown, in the last row of Table 1, data from SKA1-low and SKA1-mid (or SKA1-survey), should be combined to obtain an excellent frequency coverage and hence allow high-precision investigation of Cosmic Magnetism.

Experience from SKA1 is essential for planning further polarization observations with SKA2. However, on the basis of the above considerations, it is desirable not to have gaps in frequency range between SKA1-low and SKA1-mid (or SKA1-survey), even in the initial phases of the project. If this requirement is not initially feasible, going to slightly lower frequencies would be better for SKA1-survey PAF Band2 since a slight shift at lower frequencies would improve the Rotation Measure Synthesis resolution. Therefore, for the PAF Band2 of SKA1-survey (if the PAF Band1 will not initially available), starting from 500 MHz would be better than starting from 650 MHz.

2.2 Angular resolution

High angular resolution observations are crucial to reduce the beam depolarization. Observing an extended not uniformly polarized radio source with a resolution larger than the angular scale of coherent polarization patches, leads to a decrease of the polarization signal. The beam smooths out the polarization of the source, and the measured polarization will be less than the true source polarization. This effect is called beam depolarization and is a major effect that limits the possibility to detect polarized signal from radio sources.

With a maximum baseline of $\simeq$200 km, SKA1-mid will achieve a sub-arcsecond resolution. Spanning a similar frequency range, but with a smaller maximum baseline, SKA1-survey will reach an arcsecond resolution. These high resolutions are ideal to reduce the beam depolarization, permitting detailed magnetic field studies in several astrophysical systems. On the other hand, to study the polarization properties of particularly compact sources such as relativistic jets from supermassive black holes in AGN and even the close environments of nearby black holes, it is needed to reach ultra-high angular resolutions up to a few milliarcseconds or lower, which is feasible through very long baseline interferometry (VLBI) involving phased SKA1-mid (or SKA1-survey) and other external radio stations/arrays all around the globe. To these, the phased SKA1 array would add a more than significant increase in sensitivity than what current VLBI arrays can achieve, hence allowing for much deeper polarization and Faraday rotation maps than possible now.

At the SKA1-low frequencies, Galactic and extragalactic polarized emission is poorly known and their characteristics cannot be extrapolated directly from higher frequency measurements. Recent low resolution (several arcminutes) polarization observations performed with the Murchison Widefield Array at 189 MHz (Bernardi et al. 2013), and with the WSRT at 350 MHz in a field around the nearby spiral galaxy M31 (Gießübel et al. 2013), pointed out the apparent lack of polarized sources at low radio frequencies. Both beam depolarization and internal depolarization could generate the observed depolarization. Higher angular resolution observations are essential to reduce the beam depolarization and discriminate between beam and internal depolarization. LOFAR shows more polarized sources at higher angular resolution (Heald, private communication).

With SKA1-low it will be possible to achieve a resolution of the order of 10 arcseconds. At a redshift z=0.1 − 1, 10 arcseconds correspond to 18 − 80 kpc. Especially at the lowest frequencies, SKA1-low may not provide a sufficient resolution to overcome the beam depolarization. We therefore strongly support the possibility to have SKA1-low with longer baselines.

High angular resolution observations are also fundamental to reduce the confusion limit created by unresolved faint radio sources (Condon et al. 2012). Confusion noise will be an issue with SKA1-low after a few seconds of integration time. The only possibility to reduce the confusion limit is to reach a higher resolution.

Therefore, we support the possibility of having SKA1-low with a collecting area better distributed over longer baselines. This will permit not only reduction in the confusion limit, but also of the beam depolarization.

2.3 Field of view

SKA1 will primarily conduct surveys of large fraction of the sky, mapping spectral line, continuum, and polarization. The capability to image large field of view will be achieved both with SKA1-low ($\simeq$27 deg^2 at 110 MHz) and SKA1-survey ($\simeq$18 deg^2 at 1.67 GHz). Equipped with Phased Array Feeds (PAFs), SKA1-survey will make it possible to image a field of view about a factor 40 better than SKA1-mid ($\simeq$0.49 deg^2 at 1.67 GHz).

Interesting fields of view in the context of the Cosmic Magnetism range from arcminute to degree scales. 1 degree is e.g. $\simeq$20 Mpc at z=0.5 so relevant to cosmic web, and $\simeq$3.5 Mpc at z=0.05 so relevant to clusters of galaxies. To image structures with an angular extent larger than the field of view mosaicing observations will be necessary. But it is important to emphasize that, both the field of view and the largest angular scale detected by the interferometer (see Sect. 2.4) must be taken into account in imaging large angular scale structures.

2.4 Largest Angular Scale

The minimum baseline of an interferometer defines the maximum angular scale that it is possible to image. Interferometers filter out structures larger than the angular size corresponding to their shortest spacings and this may pose serious limits to the synthesis imaging of extended structures. This may be a critical issue (see also the talk by C. Ferrari at the SKA Continuum Assessment Workshop) in all the science cases in which it is important to image large angular scale structures (e.g. nearby galaxy clusters, galactic foreground, cosmic web). RM studies toward a large number of bright background sources do not need short baselines. However, Cosmic Magnetism studies also require imaging of large scale synchrotron emission both in total intensity and polarization. The detection of large scale structures may be a critical issue mainly in total intensity. The radio halo emission (see Sect. 4.3) at the center of nearby clusters may have, for example, an angular extension of more than 1 degree (e.g. Brown & Rudnick 2011). In polarization the structures are typically less extended than in total intensity but, Galactic polarization structures of $\simeq$ 2 degrees have been measured (e.g. Iacobelli et al. 2013).

In the Baseline Design no clear specifics are given for the minimum baseline of the SKA1-mid, SKA1-survey, and SKA1-low. This parameter should be considered in the text and specified in the

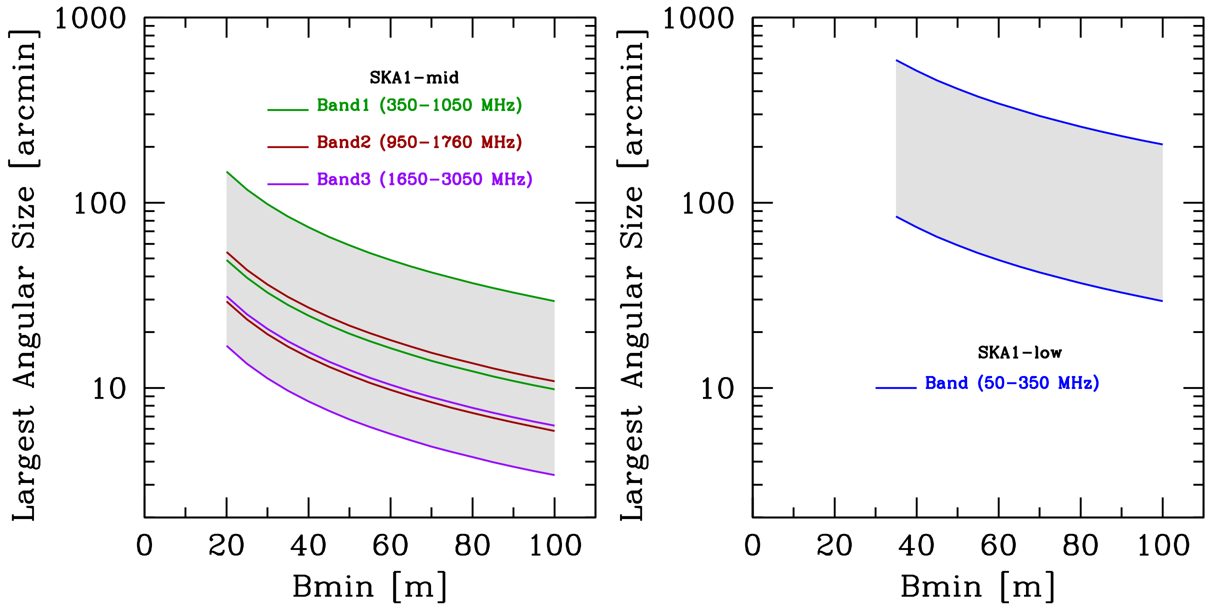

Figure 1: Largest Angular Size detectable with SKA1-mid (left) and SKA1-low (right) as a function of the minimum baseline (Bmin) of the array. The SKA1-survey's expectations are similar to those of the SKA1-mid, spanning a similar frequency range.

tables. It seems (Fig.10 of the Baseline Design) that the minimum baseline for SKA1-mid may be 30 m. The minimum baseline should be fixed. Is this value of 30 m already definitive or would a reduction of this distance it may be possible?

In Fig. 1 we show the expected Largest Angular Scale (LAS) detectable as a function of the minimum baseline (Bmin) of the array. SKA1-mid (green, red, and violet lines) is shown on the left panel, while SKA1-low (blue lines) is shown on the right panel. The SKA1-survey's expectations are similar to those of the SKA1-mid, spanning a similar frequency range of Band1 and Band2. With the SKA1-mid (and SKA1-survey) it will be difficult to recover the entire total intensity emission in structures with an angular extent larger than 1 degree, even with a very small separation between the antennas.

In the SKA1-low, if the separation between the stations is taken as small as $\simeq$35 m, the detection of structures extended 1 degree in angular size is not an issue. But, the detection of large scale structures may be compromised if larger separations between the stations are considered (e.g. $\simeq$100 m, or more).

At the center of the arrays, it is therefore recommended to reduce as much as possible the distance between dishes (SKA1-mid and SKA1-survey) and between the stations (SKA1-low). It is also recommended to consider SKA1-low stations not larger than $\simeq$35 m, achieving a large field of view and a good detection of large angular structures. We note that an increase of the size of the SKA1-low stations will reduce the field of view and will increase the minimum baseline. The latter effect may limit the possibility to detect large angular scale structures, even with mosaicing observations.

The imaging performance for possible "second generation" SKA1 configurations is under investigation by R. Braun (SKA memo in preparation). We note that the proposed SKA1-low "super-stations", composed by 8 sub-stations all of 45 m in diameter, can image large scale angular structures only if the correlation of the signal is performed between the sub-stations of the array.

2.5 Polarization Purity

Large-scale emission associated with AGN jets and resolved galaxy disks is often highly polarized at levels of a few 10s of percent. However AGN cores are more typically polarized at a few percent and the integrated emission of most galaxies is less than 1% at 1.4 GHz. Such sources will be the dominant population of the μJy radio sky. A high degree of polarization purity is fundamental to detect linear polarized signal from astrophysical sources seen down to sub-mJy levels. (We note that polarization purity is also extremely important to set the level of calibration required for the Epoch of Reionization experiment).

The polarization purity reachable with SKA1-low is unspecified in the Baseline Design. The only specification provided for SKA1-mid and SKA1-survey is given in Table 5 of the Baseline Design, where it is indicated that a polarization purity of -30dB (0.1%) is required within the HPBW. However, proper specifications for PAF system need to be more detailed than this. Information on temporal stability of instrumental polarization, and pre- and post- astronomical calibration, are missed in the Baseline Design.

We note that the cross-polarization ratio (XPR), which is the polarization purity parameter commonly used to assess the polarimetric performance, may be not suitable as a polarimetry figure of merit. This is because although the cross-polarization ratio is relevant for raw, pre-calibrated polarimetry, in general it is not relevant to the quality of the polarimetry after polarimetric calibration. However, a cross-polarization ratio can be constructed from invariants of the Jones matrix (the matrix that describes the polarimetric response of a polarimeter) that quantifies polarimetric performance even after calibration. This cross-polarization ratio is defined intrinsic cross-polarization ratio (IXR) and it is a fundamental figure of merit for polarimeters since it is a well defined quantity that directly relates to the error in post-calibration data (Carozzi et al. 2009). In the following, to address the ambiguity of "polarization purity" (whether it is pre- or post- calibrated), we refer to the post-calibration purity (or IXR), since it is more relevant to the science case.

To enable the basic cosmic magnetism goals, post-calibration polarization purity of 0.1% is required over the field of view. It is important to be able to accurately model how the polarization purity deteriorates towards the periphery of the beam, and the levels reached at the edge of the field of view should be clarified.

In addition to linear polarization, circular polarization is another important but challenging diagnostic of magnetic field and particle populations in active galactic nuclei (see e.g. O'Sullivan et al. 2013a for a review of the relevant physics and observational status). Since circular polarization is generally not modified by external screens, it can illuminate the origins of the fields down to the scale of its launching in the supermassive black hole accretion disk. Circular polarization values can be reasonably large for galactic compact objects ($\simeq$5% in the Sag A* magnetar Shannon & Johnston 2013, up to 10s of % for pulsars Radhakrishnan & Rankin 1990). But in one of the earliest compilations of circular polarization at $\simeq$1 GHz, Weiler & de Pater (1983) classified 0.1% as being strong. In order to have reasonable samples of circular polarization sources, the post-calibration purity in circular polarization should be $\simeq$0.025%.

The frequency dependence of circular polarization also carries invaluable diagnostics, so sensitive that circular polarization capabilities should be preserved at all bands. It is therefore a desirable goal to achieve a polarization purity even much better than 0.1%. In the future, observational steps on circular polarization science with pre-SKA projects will flesh out this research field and the mentioned specs will be better defined during pathfinder science projects.

2.6 Survey Speed

The survey speed of an instrument degenerates with field of view and sensitivity. SKA1-survey will primarily conduct surveys of large fraction of the sky, mapping spectral line, continuum, and polarization. Looking at Table 1 on Pag.18 of the Baseline Design, SKA1-survey is listed as having a survey speed of 2.75×10^6 deg^2 m^4/K^2. However, in the same table, SKA1-mid is listed with a survey speed of 1.30×10^6 deg^2 m^4/K^2. So SKA1-mid may reach higher angular resolution than SKA1-survey, a slightly better frequency coverage than SKA1-survey, and is only a factor of two down in survey speed. Therefore, with the current specifications SKA1-mid can do surveys almost as well as SKA1-survey.

There is an apparent similarity between SKA1-mid and SKA1-survey capabilities. We suggest to optimize some aspects of one of the two instruments for deep observations and some aspects of the other instrument for wide-field observations. An even higher survey speed is recommended for the instrument dedicated to wide-field observations.

3 Polarization surveys with the SKA1

A relatively shallow spectro-polarimetric survey over a large field of view, and very deep spectro-polarimetric surveys over small field of views performed with SKA1 at $\simeq$1 GHz on the broadest possible frequency coverage, will permit to exploit the Cosmic Magnetism in a variety of astrophysical sources and to obtain important inputs in view of the SKA Magnetism Key Science Project in the Phase-2 of SKA (Gaensler et al. 2004, Beck & Gaensler 2004).

The surveys indicated in Table 2 have been identified as suitable to address nearly all key science projects in Cosmic Magnetism studies (see Sect. 4). An additional survey at lower frequency (Band1 of the SKA1-mid) aimed to detect the polarized emission in large scale filaments in the cosmic web, and higher/wider frequency follow up on individual sources (AGN, galaxies, etc.) are under investigation.

The polarized radiation of extragalactic background sources can be used to investigate the magneto-ionic medium along the entire line of sight between us and the source of emission. The densest all-sky grid of Faraday rotation measure actually available has been obtained by Taylor et al. (2009). They analyzed the NRAO VLA Sky Survey (NVSS, Condon et al. 1998) data to derive rotation measures toward 37,543 polarized radio sources. The resulting RM catalog contains data on sources distributed roughly equally over the sky at declinations larger than -40°, with an average density of more than one RM per square degree. In the top panel of Fig. 2, is shown the all-sky map of Faraday rotation measure, while in the bottom panel of Fig. 2 is shown a reconstruction of the Galactic Faraday depth (Oppermann et al. 2012), mostly based on the Taylor et al. (2009) results.

A survey to be performed with the PAF Band2 of the SKA1-survey over a large field of view, will provide an all-sky grid of Faraday rotation measures. At μJy levels, this survey may provide an all-sky grid of Faraday rotation measures $\simeq$300-1000$\times$ denser than the RM grid based on the NVSS survey, allowing us to measure the magnetic fields in a huge number of intervening galaxies out to high redshifts, to search for a pervasive intergalactic magnetic field, and to investigate the detailed structure of the magnetic field in the Milky Way, in external galaxies and galaxy clusters. As discussed in Sect. 3.1, we acknowledge a large uncertainty in the predictions of polarized source counts at such low flux levels, but we stress that even with the more conservative estimates, the POSSUM (Gaensler et al. 2010) survey will improve over NVSS by a factor of 30-40, and SKA1 will improve by another order of magnitude.

Very deep surveys to be performed with SKA1-mid, over a relatively small area, will enable us

Table 2: Wide-band spectro-polarimetry surveys.

Instrument	Band	Field of View	Resolution	Sensitivity
SKA1-survey	PAF Band2	30.000 deg^2	$\simeq$2$''$	$\simeq$2 μJy/beam
SKA1-mid	Band3/Band2	3/10 deg^2	$\simeq$0.5$''$	$\simeq$0.075 μJy/beam

to measure the magnetic field structure and its relation to gas flows in a large number of galaxies, AGNs and galaxy clusters with unprecedented precision.

We note that to pave the way for wide-field spectro-polarimetric continuum surveys to be performed with SKA1 and SKA2, there are several polarization surveys under way or planned, e.g. GALFACTS with Arecibo (Taylor & Salter 2010), GMIMS with single-dish telescopes (Wolleben et al. 2009), LOFAR (Anderson et al. 2012, Heald et al. 2012, Beck et al. 2013), and POSSUM with ASKAP (Gaensler et al. 2010), allowing sensitive imaging of polarized radiation and Faraday Rotation Measure from both diffuse emission and against a high density number of extragalactic sources.

3.1 Polarized source counts

Little is known about the faint polarized sky. Therefore, the expected polarized source counts at μJy levels must be extrapolated from current surveys at $\simeq$1GHz.

Extrapolating from the deep survey in the GOODS-N field, at a sensitivity of $\simeq$15μJy and at a resolution of 1.6$''$, the polarization counts of sources at a flux level of $\simeq$1μJy are expected to be $\simeq$315 per square degree (Rudnick & Owen; submitted). These numbers are rather in agreement with the extrapolation derived by C. Hales (private communication), on the basis of the second data release of the Australia Telescope Large Area Survey (ATLAS DR2), at a sensitivity of $\simeq$25μJy/beam and at a resolution of 10$''$ (Hales et al.; submitted).

At a resolution of 1$'$, from NVSS polarization stacking, the expected number of polarized sources at a flux level of 1μJy results in $\simeq$1300 per square degree (Stil et al.; submitted). This extrapolation involves a first-order power law fit to fractional polarization versus flux density. Using a second order fit to fractional polarization versus flux density, one gets numbers about 30% lower than that obtained with a first order fit. Given the 30% difference between first and second order fit to the data (p $\geq$ 50 μJy), and other errors related to the extrapolation uncertainty and other aspects of the stacking process the true uncertainty can be comparable to the 50%.

The different polarized source counts predicted by the different extrapolations mentioned here may be related to several factors that should be considered:
(i) Extrapolations are performed on surveys characterized by different sensitivity and this may cause slight differences in the final results.
(ii) Extrapolations are performed on surveys at different angular resolutions. The comparison between expectations at different resolution should be performed incorporating beam depolarization models.
(iii) Extrapolations are performed by using different approaches (e.g. stack of large field of view or very deep surveys over small areas). It is worth noting that the stacking result by Stil et al. (submitted) is derived from hundreds of thousands of NVSS sources over 80% of the sky while the expected counts by Rudnick & Owen (submitted) consider a very deep but small field of view.
Finally, we note that the predictions of the number of faint polarized radio sources that can be detected with SKA1 depend on the polarization properties of radio sources with a flux density below $\simeq$1 mJy. Total intensity source counts suggest a transition in the dominant population from AGN to star forming galaxies around this flux density and the properties of brighter radio sources

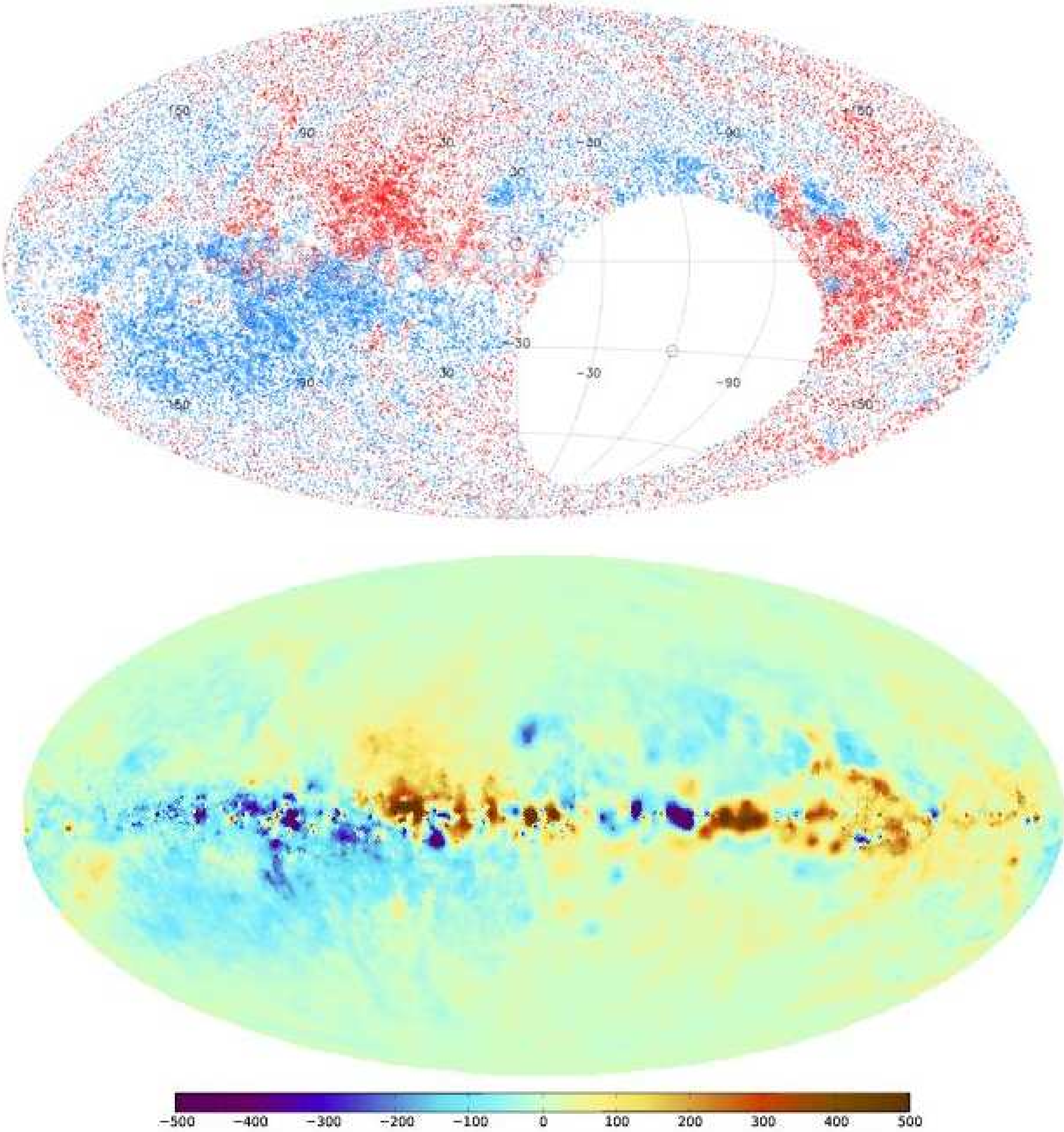

Figure 2: Top: plot of 37,543 RM values over the sky north of $\delta=-40°$. Red circles are positive rotation measure and blue circles are negative. The size of the circle scales linearly with magnitude of rotation measure (Taylor et al. 2009). Bottom: Reconstruction of the Galactic Faraday depth that summarize the current state of knowledge (Oppermann et al. 2012).

may not be representative for this fainter population. We do not yet understand the evolution of the luminosity functions, in total intensity and in polarization, and resolving this uncertainty will be one of the headline science results of future SKA1 surveys.

4 Cosmic Magnetism - Science Drivers

The science cases for SKA1-mid, SKA1-survey, and SKA1-low, are a full version of the early science programs for SKA precursors and pathfinders (ASKAP, MeerKAT, LOFAR). In particular, the densely-spaced RM grid which would result from the wide-band spectro-polarimetry surveys at $\simeq$1GHz described in Sect. 3, complemented by deep polarization observations at lower (and if possible higher) frequencies , will permit us to generate new knowledge of cosmic magnetism in the following research area:
1) *Galactic magnetic field and the magnetic foreground to extragalactic fields and the Cosmic Microwave Background (CMB).*
2) *Magnetism and galaxy evolution.*
3) *Magnetic fields and galaxy clusters formation and evolution.*
4) *Detection and characterization of the magnetic cosmic web and relation to large scale structures of matter.*

In addition, magnetic field studies will be fundamental to address the following important questions:

• *What are the properties of magnetic fields in Active Galactic Nuclei (AGN)?*
It is well known that AGN jets are highly linearly polarized (e.g. Agudo et al. 2010), and that the magnetic field threading them must play a key role on both the formation and collimation of the jet, as well as on its dynamics both on the small scales and at large scales. However, despite decades of study, there are still several relevant open questions that need to be solved to understand both the AGN and the jet phenomenon. Some of these questions include: What is the actual geometry and intensity of the magnetic field on this kind of sources? Where are these magnetic fields dragged from? How are they actually dragged into the jet? How is the magnetic field controlling the jet formation phenomenon? Most of these open questions are related to the properties of the innermost regions of jets, close to the supermassive black holes that produce them, where the strongest Faraday rotation takes place (e.g. Zavala & Taylor 2004, Asada et al. 2008, Gómez et al. 2011, Agudo et al. 2012). Therefore, studying these problems requires ultra-high resolutions up to several milliarcseconds or less, that are technically feasible by connecting a phased SKA array (either the full instrument or part of it) with other radio stations or arrays. Moreover, synchrotron self-absorption, which reduces its effect with increasing frequency (e.g. Lobanov 1998, Hada et al. 2011), prevents to observe the innermost regions of relativistic jets, where these are still being formed and collimated, if observations are performed at frequencies much lower than $\simeq$20 GHz.

Moreover, since jets in AGN are so abundant and so powerful sources of linearly polarized radiation all over the sky, they are ideal background sources to perform Faraday rotation studies to check the foreground Galactic (and even intergalactic, e.g. in galaxy cluster media) magnetic fields and free electron content. Clearly, using AGN jets as a tool to study foreground properties work better if having an as detailed as possible knowledge of the polarization properties of the former.

• *What is the relationship between supermassive black holes and their environments?*
The broadband Faraday structure and depolarization of extragalactic sources provides a unique and extremely sensitive probe of the thermal environments of radio galaxies and AGN, addressing

key questions on entrainment, feedback and triggering. Pentericci et al. (2000) found that the fraction of radio galaxies with extreme Faraday rotation increases at larger redshifts, likely because of the increasing density of the environment. Such observations also stimulate work on the cosmic origins of magnetic fields; Beck et al. (2013) e.g., explore the seeding of protogalactic magnetic fields through supernova explosions, while Bonvin et al. (2012) look further back at magnetic field generation possibilities from inflation. At low redshifts, O'Sullivan et al. (2013b) have found a possible detection of thermal material mixed throughout the relativistic lobe plasma in Centaurus A. A comprehensive survey of AGN and radio galaxies at all luminosities, redshifts and environments is needed to understand the thermal content, magnetic structure, and even magnetic field origins as galaxies form and evolve.

• *How do galaxies and structures evolved over cosmic time?*
A broadband polarized SED allows us to apply a "polarization k-correction" and shift every polarization measurement into the rest-frame of the emitter (provided we have redshifts from spectroscopy or photo-z's), allowing us to infer the magneto-ionic properties of AGN, galaxies and their immediate environments, as well as the overall evolution of magnetic fields in the IGM. We now have exciting samples of RM vs z (e.g. Hammond et al. 2012), but any analysis is severely limited by our inability to correct each data point for cosmological expansion. A broadband data set would allow us to look at the evolution of rest-frame properties as a function of cosmic time.

• *What are the physical properties of absorbing systems?*
Broadband Faraday rotation allow us to uniquely determine sophisticated aspects of L* galaxies such as their covering fraction and degree of turbulence. Bernet et al. (2012) have shown than even a simple model can provide enormous new insight into the nature of the invisible intervening population seen against polarized background sources, but only if there is broadband frequency coverage. We will use the data obtained over the broadband frequency coverage of SKA1-mid, SKA1-survey, and SKA1-low to test and improve such models. As shown by Bernet et al. (2013), high resolution in Faraday space is needed to understand the nature of intervening systems.

The connecting point for all the Cosmic Magnetism experiments proposed here is that there are enormous degeneracies between different types of Faraday rotation / depolarization behavior (see e.g. O'Sullivan 2012). These degeneracies can only be broken by a broadband frequency coverage. If we want to go from Faraday rotation and polarization data to physical information, we need the resolution, the sensitivity, and the large coverage in λ^2 provided by SKA1-mid, SKA1-survey, and SKA1-low. In addition, proper interpretation of the results will require extensive testing of the algorithms used to accurately extract the polarization and RM properties.

4.1 Galactic magnetism

Interstellar magnetic fields play a crucial role in our Galaxy: they govern the structure and the dynamics of the interstellar medium, they regulate the process of star formation, they accelerate cosmic rays and confine them to the Galaxy, they provide a heating source for the halo through magnetic reconnection. It is, therefore, very important to accurately determine their spatial structure at large and small scales, including the field strength distribution, the overall magnetic topology, the azimuthal structure (axisymmetric, bisymmetric or more complex) and vertical parity (symmetric, anti-symmetric or a combination of both) of the large-scale magnetic field, the number and radial locations of field reversals in the Galactic disk, the possible connection between the magnetic field in the disk, in the halo and near the Galactic center. All these properties are also relevant to the theoretical question of the origin and evolution of Galactic magnetic fields, and their observational determination will make it possible to place serious constraints on the dynamo scenario as well as on specific Galactic dynamo models.

RMs of compact extragalactic sources can be used to derive a detailed description of Galactic magnetic fields. In Fig. 3 is shown a sketch of the large-scale magnetic field in the disk of the Galaxy derived from Faraday rotation measures of pulsars and extragalactic sources (Brown 2010). However, the sparse sampling of current RM data sets prevents a detailed analysis on scales smaller than 1 degree (e.g. Taylor et al 2009). The densely-spaced RM grid which would result from the SKA1 surveys at $\approx$ 1 GHz proposed in Sect. 3 will overcome the actual observing limitations permitting a detailed study of the Galactic magnetic field at high resolution. In addition, the broad frequency coverage of SKA1 will allow detailed RM Synthesis of the diffuse synchrotron emission of the Galaxy (see Table 1). Current capabilities using e.g. LOFAR miss (Faraday thick) components in Faraday depth due to limited frequency coverage and sensitivity. However, with SKA1 we will be able to exquisitely map this polarized emission, enabling charting synchrotron emissivity in 3D and investigate small-scale magnetic field patterns (Iacobelli et al 2013).

The combined RM grid and RM Synthesis will make it possible to distinguish between local foreground structures and the overall configuration of the large-scale magnetic field in the Milky Way. A comparison with theoretical dynamo (or alternative) models will then shed light on the magnetic field amplification mechanisms. For instance, the detection of bisymmetric or quadrisymmetric azimuthal modes may point to the influence of an external disturber or to the impact of the gaseous spiral-bar structure, respectively (e.g. Ferrière 2007). Similarly, the detection of antisymmetric vertical modes may be indicative of strong dynamo action in the Galactic halo (e.g. Moss & Sokoloff 2008, Moss et al. 2010, Gressel et al. 2008). Another important diagnostic tool is the exact number and locations of field reversals. Radial reversals can easily be produced by a galactic dynamo, even if the dynamo-amplified field is axisymmetric – in the latter case, radial reversals naturally arise when the large-scale rotational velocity has a strong vertical gradient (Ferrière & Schmitt 2000). Alternatively, radial reversals could be a long-lived transient phenomenon following an early injection of small-scale fields (Hanasz et al. 2009, Moss et al. 2012). Field reversals could also occur along the vertical, as predicted by Machida et al.'s (2013) numerical simulations of galactic dynamos driven by the magnetorotational and Parker instabilities. These simulations lead to other interesting predictions, such as quasi-periodic reversals of the azimuthal field on timescales $\sim$ 1.5 Gyr (see also Nishikori et al. 2006).

On small scales, the Galactic magnetic field structure is known to be complex. The magnetic field is constantly pushed around, amplified and diffused by supernova explosions, shock waves, jets and other dynamical processes in the Milky Way. However, this turbulent magnetic field also provides important feedback on these gas motions such as transport of gas and energy from the star forming disk to the Galactic halo, and the propagation and acceleration of cosmic rays, as shown by energy equipartition arguments (Heiles & Haverkorn 2012). The densely-spaced RM grid and high-resolution RM synthesis data will also be a powerful probe of turbulence. Structure function analysis will become possible in exquisite detail to investigate the variation of turbulent parameters within the Milky Way. The existence of these variations is shown in current results of structure function analysis for a RM grid in the Galactic plane, which have shown that the outer scale of fluctuations varies between spiral arms and inter-arm regions (Haverkorn et al. 2008). Also, Stil et al. (2011) presented RM structure functions for the entire northern sky and showed that there is a distinct asymmetry between the northern and southern Galactic hemispheres, which was also noted in Mao et al (2010) who studied RM grids towards the Galactic poles. Stil et al. (2011) also pointed out the importance of local foreground structures such as supernova remnants or HII

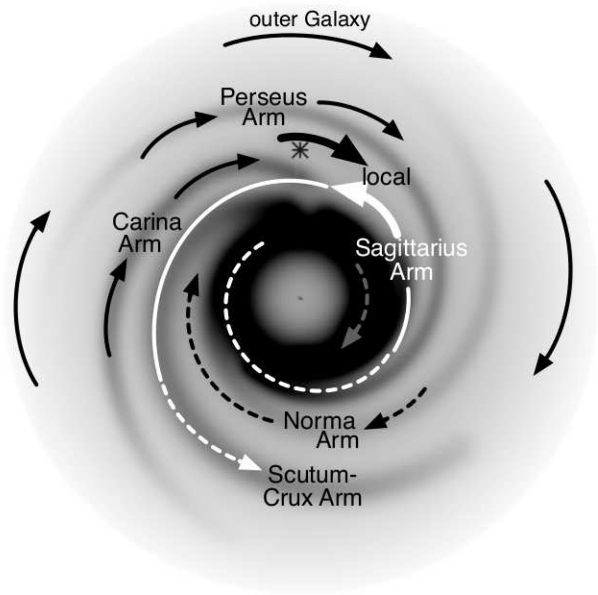

Figure 3: Sketch of the large-scale magnetic field in the disk of the Galaxy based on Faraday rotation measures of pulsars and extragalactic sources. Bold arrows show only accepted magnetic filed directions. The remaining solid and dashed arrows still need confirmation (from Brown 2010).

regions on the RM grid, which can be studied and/or subtracted much better in a densely spaced grid.

The Galactic magnetic field is a key ingredient to understand not only the physics of the interstellar medium but also some aspects of cosmology. Being able to model the Galactic magnetic field is very important for accurate foreground subtraction to address some key sciences in the 21th century astrophysics and cosmology: For "CMB polarization", which is a direct and concrete evidence to prove the inflation theory, a detailed rendering of polarized foregrounds is key; the "Epoch of Reionization" project, which is a precious record telling us when and how the first stars and first galaxies were formed, needs exquisite polarization purity and knowledge of polarized foregrounds in order to correct for these; finally, the "Origin of Ultra-High Energy Cosmic Rays" is a longstanding unknown of our universe, which can only be solved with a reliable and accurate magnetic field model of the Milky Way.

4.2 Magnetism in external galaxies

Magnetic fields in nearby external galaxies can be studied by imaging polarimetry of synchrotron emission and by analyzing rotation measures of polarized background sources.

High-resolution imaging of magnetic fields in spiral galaxies require a major increase in sensitivity of observations, which will be achieved by the SKA1. In this way the detailed structure of the magnetic fields in the ISM of galaxies and in galaxy halos can be observed and the magnetic power spectra measured. Direct insight into the interaction between gas and magnetic fields will become possible. The simulation by Moss et al. (2013) gives an idea how complex magnetic fields in spiral galaxies probably are and why much higher resolution is needed with SKA1.

If diffuse polarized emission is too weak to be detected, the method of RM grids towards

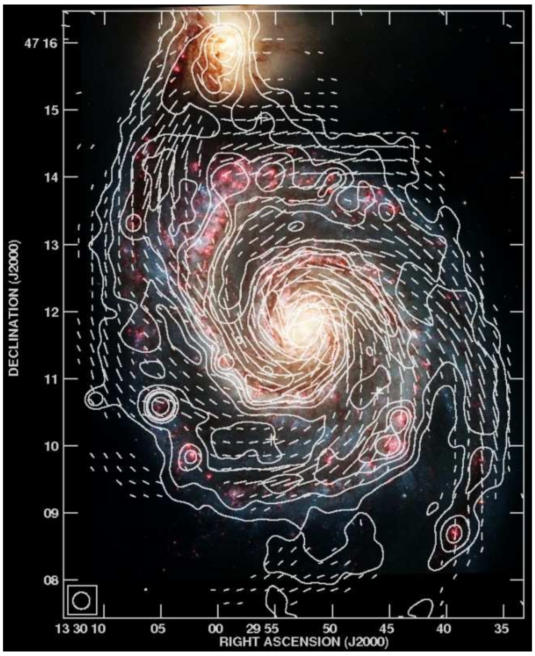

Figure 4: Spiral galaxy M51. Total radio intensity (contours) and B-vectors at 4.8 GHz, combined from observations with the VLA and Effelsberg 100-m telescopes (Fletcher et al. 2011). The background optical image is from the HST (image credit: NASA, ESA, S. Beckwith (STScI), and The Hubble Heritage Team (STScI/AURA)).

background QSOs can still be applied and allows us to determine the field strength and pattern in the intervening objects, such as distant spiral galaxies. However, we note that if background quasars are used to probe the magnetic fields of intervening objects, it should be taken into account that they can display extremely large RM produced in their cores (Zavala & Taylor 2004). Indeed, Taylor et al. (2009) report RM of up to $\simeq$100 rad/m^2 or larger for a fraction of sources far from the Galactic plane, which may be a problem for accurate studies of the magnetic field properties of the intervening systems if the contribution of the background and the intervening sources are not disentangled. Such large RM can prevent from any reliable measurement of the true polarization properties of the intervening objects unless there is an accurate estimate of the actual RM of the background source. For such high RM, it is desirable to measure the polarization properties of background + intervening object at the highest possible frequencies in order to disentangle between them.

Imaging of synchrotron emission from nearby spiral galaxies (see e.g. Fig. 4) shows that most spiral galaxies have a ordered spiral magnetic field in the plane of the disk (e.g. Beck & Wielebinski 2013). The symmetry of the magnetic field and its projection on the sky imply that an unresolved face-on spiral galaxy is typically unpolarized. On the other hand, for an inclined galaxy, the azimuthal magnetic field increasingly projects along the apparent major axis of the disk. Thus, an unresolved inclined spiral galaxy is polarized with the plane of polarization (B rotated by 90°) along the minor axis (Stil et al. 2009). Therefore, polarization measurements with the SKA1, of unresolved spiral galaxies will allow to derive in a statistical way properties of the magnetic fields in disk galaxies using large samples in the local universe and at high redshift. This is also of interest for gravitational lensing experiments because the plane of polarization is an invariant, hence recording in a statistical way, the original minor axis of a lensed galaxy.

Dynamo theory presently is the best-developed model for field evolution in galaxies. It predicts timescales of amplification and coherent ordering of magnetic fields in galaxies. Based on models describing the formation and evolution of dwarf and disk galaxies, the probable evolution of turbulent and regular magnetic fields can be tested observationally (see Arshakian et al. 2009), with the means of synchrotron emission and Faraday rotation in intervening galaxies against background sources:

− Strong isotropic turbulent fields (in equipartition with turbulent gas motions) and hence unpolarized synchrotron emission are expected in galaxies at $z<10$.

− Strong regular fields (which are coherent over a scale of about 1 kpc) and hence polarized synchrotron emission and fluctuating RMs are expected in galaxies at $z\leq3$.

− Large-scale patterns of fully coherent regular fields and hence polarized synchrotron emission and large-scale RM patterns are expected in dwarf and Milky-Way type galaxies at $z\leq1$.

− Giant galaxies (disk radius>15 kpc) may not yet have generated fully coherent fields.

− Major mergers enhanced turbulent fields, but destroyed regular fields and delayed the formation of fully coherent fields. The lack of regular fields in nearby galaxies can be a signature of major mergers in the past.

Radio continuum and far-infrared flux densities are tightly related in galaxies of the local universe. Unpolarized synchrotron emission from starburst galaxies, signature of turbulent magnetic fields, should be detected with the SKA1 out to large redshifts, depending on luminosity and magnetic field strength. However, for fields weaker than $3.25(1+z)^2\mu$G, energy loss of cosmic-ray electrons is dominated by the inverse Compton effect with CMB photons, so that the energy mostly goes to X-rays, not to the radio range. The redshift where the radio – far-infrared correlation breaks down tells us about the magnetic field evolution in the early universe (Schleicher & Beck 2013).

4.3 Magnetic Fields in Galaxy Clusters

The presence of μG-level magnetic fields associated with the intracluster medium of galaxy clusters is now widely acknowledged. Information on the intracluster magnetic fields can be obtained, in conjunction with X-ray observations of the hot gas, through the analysis of the rotation measure of radio galaxies lying in the background or embedded within the magnetized intracluster medium.

Magnetic fields can be investigated statistically by analyzing the RM of radio galaxies as a function of their projected distances from the cluster center, in galaxy clusters samples (e.g. Clarke et al. 2001, Johnston-Hollitt 2003). In addition, detailed high resolution RM images of extended cluster radio galaxies are now available, permitting studies focused on single clusters (e.g. Eilek & Owen 2002, Taylor et al. 2007, Guidetti et al. 2008, Guidetti et al. 2010, Bonafede et al. 2010, Vacca et al. 2012, Pratley et al. 2013). In general, the RM distributions seen across the radio galaxies present patchy structures. The observed RM fluctuations may indicate that the intracluster magnetic field is not regularly ordered but turbulent on scales ranging from tens of kpc to $\leq$100 pc (but see Rudnick & Blundell 2003 for a different viewpoint). By analyzing the RM of radio galaxies located at different projected distance from the cluster center, it is possible to investigate the radial decrease of the magnetic field with the thermal gas density (e.g. Dolag et al. 2001). However, the sensitivities of the current facilities limit the RM studies to a few radio galaxies per cluster.

The analysis of the polarization properties of spiral galaxies in galaxy clusters may also provide a complementary approach to obtain information on cluster magnetic fields. Indeed, the asymmetric polarized intensities of spiral galaxies observed in the Virgo cluster (Vollmer et al. 2007, Weżgowiec

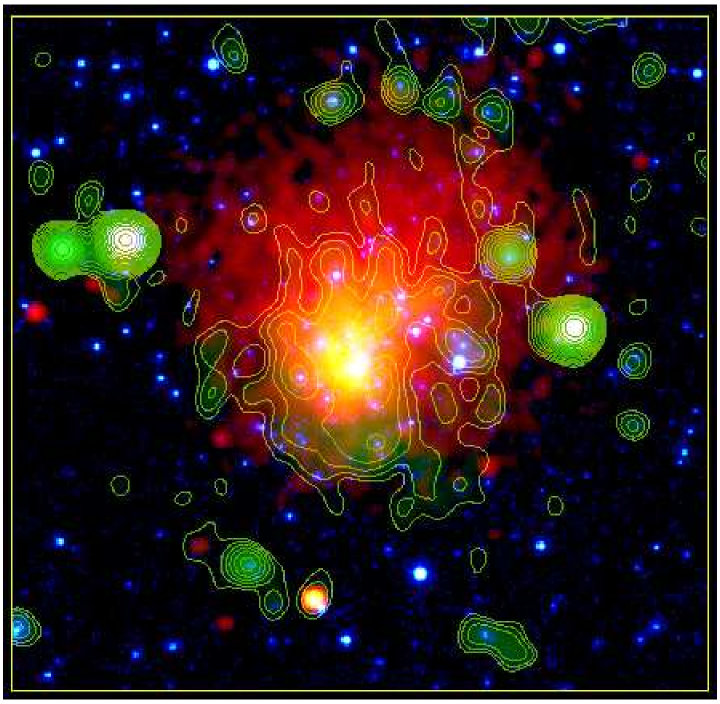

Figure 5: Galaxy cluster A665 at different wavelengths: optical (blue), X-ray (red), and radio (green contours). The radio image, showing an extended diffuse radio halo at the cluster center, has been obtained with the VLA at 1.4 GHz (Vacca et al. 2010).

et al. 2007), may indicate that the intracluster field has a radial pattern (Pfrommer & Dursi 2010).

The SKA1 surveys at ≃1 GHz described in Sect. 3 will have the potential of measuring the RM toward a large number of sources in the background or embedded within the magnetized intracluster medium, permitting derivation of a detailed description of the strength, structure, and radial decrease of cluster magnetic fields (Krause et al. 2009, Bogdanovic et al. 2011). Dedicated software tools and semi-analytical approach have been developed to constrain the magnetic field power spectrum parameters on the basis of the RM images (Enßlin & Vogt 2003, Murgia et al. 2004, Laing et al. 2008, Kuchar et al 2011).

In recent years, there has been growing evidence for the existence of cluster large-scale diffuse radio sources, of synchrotron origin, which have no optical counterpart and no obvious connection to the cluster galaxies, and are therefore associated with the intracluster medium (e.g. Feretti et al. 2012, Ferrari et al. 2008). These steep-spectrum diffuse sources are typically grouped in halos, relics and mini-halos, according to their location in the cluster and to the cluster type (merging or cool-core). The high resolution ($\simeq 1''$) of SKA1-mid and SKA1-survey will be fundamental to argue spatial structures and to investigate the spatial correspondence between the radio and X-ray emission as done in the case of the Coma cluster. Although the diffuse synchrotron radio emission of the Coma cluster had been studied extensively for decades, the combination of increased sensitivity and resolution (e.g. Brown & Rudnick 2011) was critical in identifying a previously unknown shock at the western edge of the halo, confirmed with Planck S-Z measurements (Planck Collaboration 2013) and in X-rays (Markevitch 2010). The radio and X-ray comparison is also very helpful to study cosmic ray accelerations and magnetic-field distributions.

Finally, the wide-frequency coverage of SKA-low, SKA1-mid, and SKA1-survey will be necessary to measure the halo, relics, and mini-halo spectral index correctly. Spectra at low frequencies are the key to investigate the origin of radio emissions, disentangling between different models of emission. A few more details on radio halos, relics, and mini halos are given in the following.

Radio Halos

Radio halos (Fig. 5) permeating the center of merging galaxy clusters, provide the most spectacular and direct evidence of the presence of relativistic particles and magnetic fields associated with the intracluster medium. These cluster synchrotron sources are diffuse in the intracluster medium and extend on up to Mpc scales, revealing averaged magnetic fields of $\sim 0.1{-}1$ μG spread over large volumes of space. Radio halos are typically found in clusters that display significant evidence for an ongoing merger. Recent cluster mergers were proposed to play an important role in the reacceleration of the radio-emitting relativistic particles, thus providing the energy to these extended sources. There are two main classes of models proposed to explain the origin of radio halos:(1) primary models, in which relativistic electrons are re-accelerated in situ through second-order Fermi mechanism by turbulence developing during cluster mergers (e.g. Petrosian 2001, Brunetti 2011).(2) secondary or hadronic models, in which relativistic electrons originate from hadronic collisions between relativistic protons in the intracluster medium and thermal ions (e.g. Blasi & Colafrancesco 1999, Pfrommer & Enßlin 2004a, Keshet & Loeb 2010, Enßlin et al. 2011).

The detection of polarized emission from radio halos has been shown to be extremely important to constrain the clusters magnetic field power spectrum (Murgia et al. 2004, Govoni et al. 2006, Vacca et al. 2010). However, detecting this polarized signal is a very hard task with the current radio facilities and so far only a few radio halos have been imaged in polarization (Govoni et al. 2005, Pizzo et al. 2011, Bonafede et al. 2009a).

Govoni et al. (2013), used cosmological magnetohydrodynamical simulations by Xu et al. (2012) to predict the expected total intensity and polarized surface brightness of radio halos at 1.4 GHz, under the equipartition assumption and a reasonable shape for the relativistic electron energy spectrum. At $\simeq$1 GHz, a sensitivity of $\simeq$1 μJy/beam should permit to detect, at $\sim$arcsec resolution, the polarized emission of the most powerful ($L_{1.4GHz} > 10^{25}$ Watt/Hz) radio halos.

The detection of polarized emission from radio halos may be the key to investigate the magnetic field power spectrum in galaxy clusters and to find merger shocks in the intracluster medium not visible in the X-ray images. Indeed, merger shock with Mach numbers $M \simeq 1 - 2$, do not produce enough heating to be visible in X-ray images. But, through their compression, they may get picked up in polarization (even before they get picked up in total intensity) when observed with SKA1.

Radio Relics

Relics are elongated large-scale diffuse radio emissions located in the outskirts of some galaxy clusters. They have a steep radio spectrum and are typically strongly polarized, with fractional polarizations up to $30{-}50\%$ (Fig. 6).

The relic origin is still unclear, but given their morphology and their high level of polarization, there is a common consensus that they are related to merger shocks (e.g. Enßlin et al. 1998, Roettiger et al. 1999, Enlin & Gopal-Krishna 2001, Hoeft & Brüggen 2007, Enßlin & Brüggen 2002, Kang et al. 2012, Iapichino & Brüggen 2012). The basic physical picture is that as shock fronts propagate through the intracluster medium, they accelerate particles to relativistic energies and compress magnetic fields. The details of acceleration at merger shocks are, however, not well understood. Two main mechanisms for the acceleration of electrons have been proposed to explain radio relics: (i) adiabatic compression of fossil radio plasma by the shock wave or (ii) diffusive shock acceleration by the Fermi-I process.

At the resolution of SKA1 radio relics will be studied, both in continuum and polarization, in great detail. In particular, the exquisite sensitivity and broad coverage in λ^2 space (which

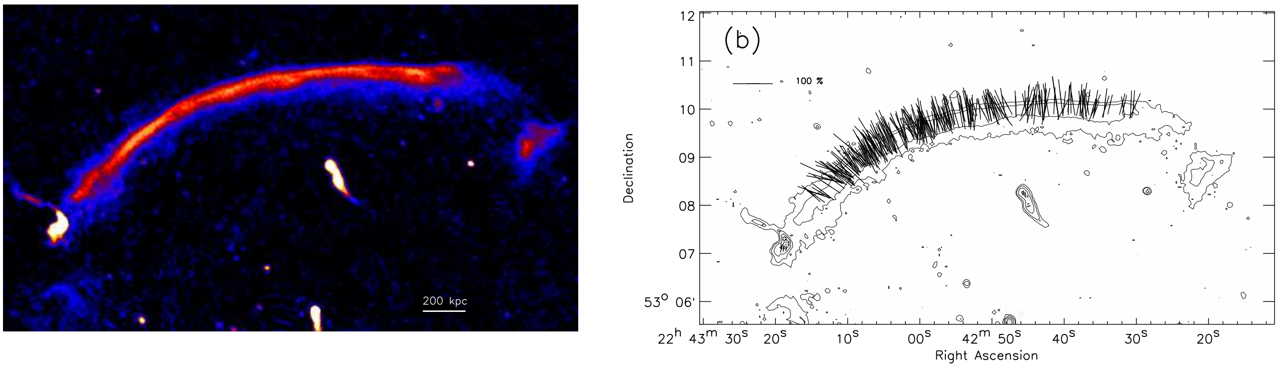

Figure 6: Left: GMRT radio image at 610 MHz of the relic in the galaxy cluster CIZA J2242.8+5301. Right: Polarization electric field vector map, obtained with the VLA at a frequency of 4.9 GHz. The E-vectors are overimposed on the GMRT observation shown on the left (van Weeren et al. 2010).

provide high resolution in Faraday space) of SKA1-mid, SKA1-survey, and SKA1-low, will allow measurement of the subtle variations in RMs across the relic sources permitting investigation of the magnetic field power spectrum at the relics location.

Relics may provide a powerful tool to trace cluster merger shocks in deep observations over the entire range of frequencies covered by SKA1-mid, SKA1-survey, and SKA1-low. The presence of intense filamentary structures detected in some relic sources like in A3667 (Johnston-Hollitt 2003) or in A2256 (e.g. Brentjens 2008, Rudnick 2011, van Weeren et al. 2012a) are not likely unique to these clusters but rather would be expected to be a common property of merging clusters when observed with good dynamic range and at high enough resolution.

In some cases (e.g. Johnston-Hollitt 2003, Clarke & Ensslin 2006, Bonafede et al. 2009b, van Weeren et al. 2010, van Weeren et al. 2012b), spectral index gradients can now be mapped as a function of distance from the shock front. These observations are very important since potentially the synchrotron spectrum gives information on the efficiency of the acceleration of the emitting electrons. However, for better understanding the acceleration of the electrons, it is necessary the high resolution of SKA1 to well-enough resolve there structures and get clear measures of the electron spectrum.

Radio Mini-halos

Some relaxed, cool-core, galaxy clusters exhibit signs of diffuse synchrotron radio emission that extend far from the dominant radio galaxy at the cluster center, forming a so-called mini-halo. Mini-halos are extended on a moderate scale ($\simeq$ 500 kpc) and, in common with halos and relics observed in merging clusters of galaxies, have a low surface brightness and steep spectrum.

The origin of mini-halos is still poorly known. It has been proposed that the cosmic ray electrons responsible for the radio emission result from a relic population of relativistic electrons re-accelerated by turbulence in the intra-cluster medium associated with the cooling flow (Gitti et al. 2002) or generated by the sloshing of the cool core gas (e.g. Mazzotta & Giacintucci 2008; ZuHone et al. 2013). On the other hand, secondary models have also been suggested to explain the radio mini-halo emission (e.g. Pfrommer and Enlin 2004b, Keshet & Loeb 2010). Fujita et al. (2007), also proposed that the cosmic ray protons producing the secondary electrons are accelerated at shocks around the central active galactic nuclei in clusters.

Radial profiles of mini-haloes can be analyzed in comparison with theoretical models to inves-

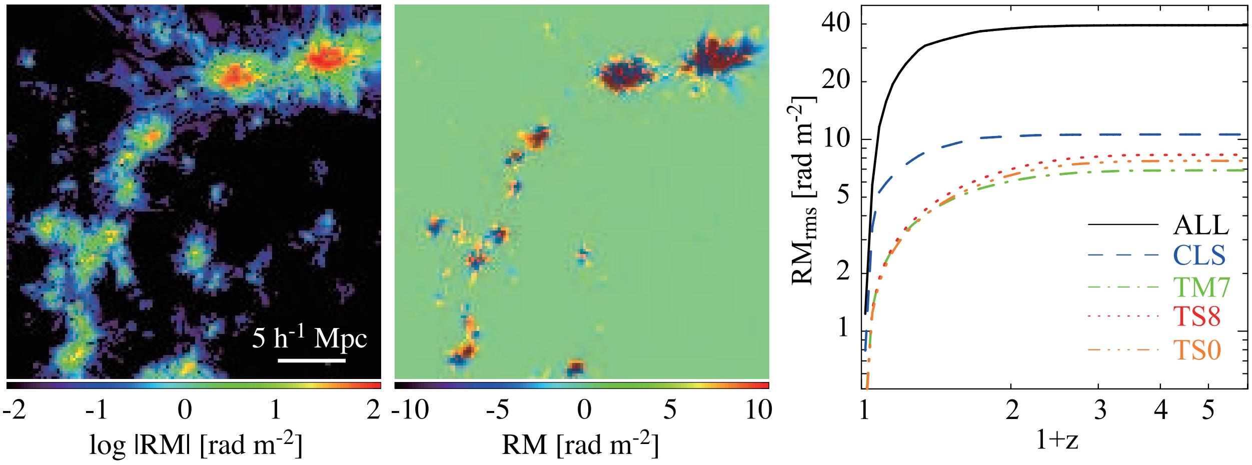

Figure 7: Left and middle: Log and linear maps of RM of $(28\ h^{-1}\mathrm{Mpc})^2$ area in the local universe of depth of $L = 100\ h^{-1}$Mpc (Akahori, Ryu 2010). Right: The rms value of RM integrated up to the redshift depth $z = 5$ (Akahori, Ryu 2011). The results with different methods for subtractions of galaxy clusters are shown as different colors.

tigate the distribution of cosmic rays and magnetic fields (Murgia et al. 2009). Fujita & Ohira (2012, 2013), compared the radial profiles presented in Murgia et al. (2009) with their model. They predicted the radial profiles of the resultant synchrotron radiation from secondary electrons created through proton-proton interaction, assuming that radiative cooling of the intra-cluster medium is balanced with the heating by cosmic ray streaming in the central regions of cool core clusters. Deep SKA1 observations will permit us to analyze the radial profiles for many other new clusters containing mini-halos, allowing us to disentangle between different models of mini-halo formation and argue how far the radio emission (thus distributions of cosmic rays and magnetic fields) is continued below the sensitivities reachable with the current instruments.

Finally, the sensitivity and the resolution of SKA1-mid and SKA1-survey will permit to investigate in detail also the mini-halos polarization and the possible association between polarization and sloshing cold fronts in clusters. These are situations where there has been a cluster merger, but the system isn't relaxed yet, and the cool gas in the core is still "sloshing" around the gravitational potential minimum, setting up cold fronts at its boundary (i.e., discontinuities in temperature and density, but not in pressure - they are not shocks). Simulations show (e.g. Ascasibar & Markevitch 2006, Roediger et al. 2011) that there should be shear motions at these boundaries, that would then stretch/align the magnetic field, and show up in polarization with the possible associated mini-halos.

4.4 Magnetic Fields in the Cosmic Web

Magnetic fields are ubiquitous even in the cosmic web of our Universe. The cosmic web is thought to be filled with the intergalactic magnetic field (IGMF), which plays essential roles in various subjects of astrophysics. For example, the IGMF imprints its own existence in the spectrum of cosmic microwave background (e.g., Yamazaki et al. 2012), deflects propagation of ultra-high energy cosmic rays (e.g., Das et al. 2008; Takami et al. 2009), and induces γ-ray halo/echo phenomena (e.g., Takahashi et al. 2011, 2012). In galaxy clusters, the IGMF attracts cosmic rays and causes synchrotron radio emissions (e.g., Feretti et al. 2012). The IGMF would be important to understand thermal balance in cool-core clusters (e.g., Fujita et al. 2012, 2013) and structures of merging clusters (e.g., Asai et al. 2005, Takizawa et al. 2008). Moreover, the IGMF could impact on the configuration of magnetic fields in spiral galaxies (Sofue et al. 2010).

The IGMF in the cosmic web could be generated by diverse mechanisms in different epochs (e.g., Ryu et al. 2012; Widraw et al. 2012 for reviews). Seed magnetic fields of any origins could be amplified through compression and eddy cascading (turbulent dynamo) in the cosmic web (e.g., Ryu et al. 2008, Dubois and Tessier 2008). Another undoubtable sources of the IGMF are leakages of the fields from galaxies through jets, supernovae, etc (e.g., Donnert et al. 2009, Xu et al. 2009, Stasyszyn et al. 2010). A conservative range of the IGMF in filaments would be $O(1-100)$ nG.

Measuring RMs of extragalactic polarized sources is one of only a few possible methods to study the IGMF. Naively, an extrapolation of radial profiles of cluster RMs (e.g., Govoni et al. 2010) may imply RM of $O(1-10)$ rad m^{-2} for filaments connecting to clusters. Akahori and Ryu (2010, 2011) predicted that the IGMF of $O(100)$ nG (Ryu et al. 2008) produces RMs of $1-10$ rad m^{-2} through filaments (See Fig. 7). Such RMs could be substantially contributed to observed RMs toward high Galactic latitudes, based on the fact that known Galactic contribution alone is not enough to explain the standard deviation of observed RMs (Akahori et al. 2013). In addition to this prediction, it is interesting to noted that Leahy (1987) and Schnitzeler (2010) independently estimated that the amplitude of RM variations across extragalactic radio sources at high Galactic latitudes is 6 rad m^{-2}.

In the SKA1 era, we will find millions of extragalactic polarized sources. Many of them may be suited to the studies of magnetic fields associated with AGNs, radio lobes, and intervening galaxies. On the other hand, it would be also true that some sources do not have large RMs and some of the lines-of-sight (LOSs) toward them do not pass through intervening galaxies. We may find such LOSs based on the properties of Faraday depolarization and/or no optical absorption counterpart. Such LOSs are suited to the study of RMs due to the IGMF, and we could study them by statistical approach with high-pass filters, or synthesis approach with Faraday RM Synthesis. The proposed SKA1 surveys at $\simeq 1$ GHz are ideal for both approaches, providing both large samples and wide frequency coverage.

A large number of extragalactic polarized sources will improve previous statistical studies of RM. For example, a high-pass filter has been employed to subtract the Galactic contribution, called residual RM. Studying the latitude dependence of RM is useful to estimate the standard deviations of RM for the Galactic and extragalactic contributions (Schnitzeler 2010). The correlation between RMs and redshifts of the sources is powerful to discriminate between possible contributions (Bernet et al. 2012, Hammond et al. 2012). Discussion of the structure function of RM provides information of the structure of the IGMF (Mao et al. 2010, Stil et al. 2011, Akahori et al. 2013). Alternatively, the two-point correlation of RMs (Kolatt 1998) and the cross-correlation between RMs and galaxies (Xu et al. 2006, Stasyszyn et al. 2010) as well as between synchrotron emissions and galaxies (Brown et al. 2010) could also provide constraints on the structure of the IGMF.

Ultra-wide band data enable us to put Faraday RM Synthesis (Section 1.1) to practical use for exploring the IGMF. The strategy to explore the RM due to the IGMF with Faraday tomography was recently studied (Akahori et al. submitted, Ideguchi et al. 2013). Further improvements of Faraday tomography such as RM CLEAN (Heald 2009) and QU-fitting (O'Sullivan et al. 2012) as well as understanding ambiguities on Faraday tomography (Fransworth et al. 2011, Kumazaki et al. submitted) are helpful for the study of the IGMF. For the study of the IGMF we suggests frequencies as low as possible to maximize λ^2 coverage. In Fig. 8 we show for example that 500-1500 MHz would be much better than $650-1670$ MHz (Ideguchi et al. 2013). The best choice would be $350-1350$ MHz, since we could combine data from SKA1-low and SKA1-survey (or SKA1-mid) without any gaps in frequency (Section 2.1).

Finally, the detection of the synchrotron emission of the cosmic web is another important science

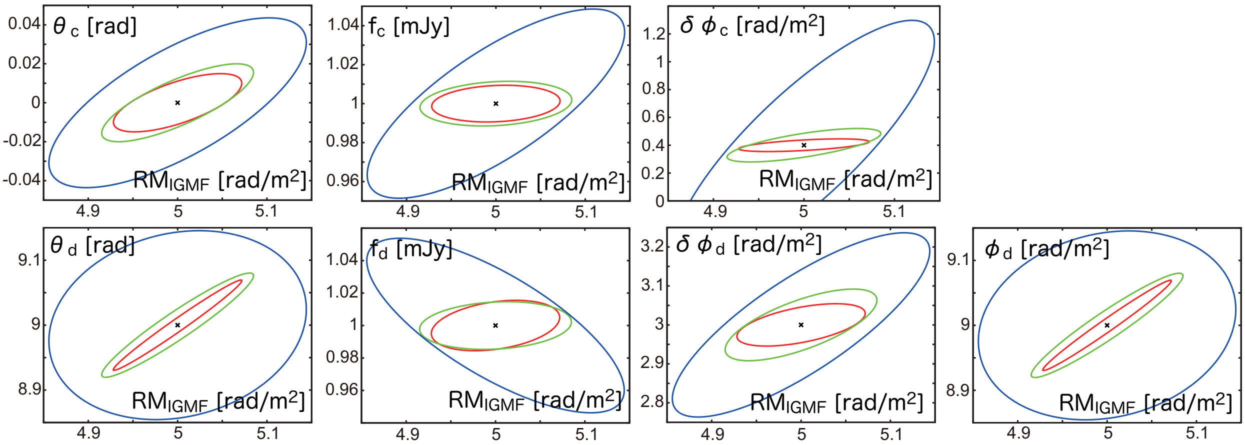

Figure 8: Results of Fisher analysis on QU-fitting (we fit mock Stokes Q and U with those calculated from the model Faraday dispersion function with eight model parameters). Contours show the $3-\sigma$ confidence regions of the model parameters, where we consider observations of 1 mJy source viewed through RM due to the IGMF of 5 rad m^{-2} and Galactic diffuse emissions of 1 mJy (see Ideguchi et al. 2013 for details of the model). Color lines show the cases with $650-1670$ MHz (blue), $500-1500$ MHz (green), and $350-1350$ MHz (red), respectively, for SKA1-survey. Lower frequency coverage gives better results.

case for cosmic magnetism. The low-frequency reachable with SKA1 have the potential to map the steep-spectrum, cosmic-web of synchrotron emission, illuminating large-scale magnetic fields in the Universe.

5 References

Agudo, I., Thum, C., Wiesemeyer, H., Krichbaum, T.P., 2010, ApJS, 189, 1
Agudo, I., Gómez, J.L., Casadio, C., et al., 2012, ApJ, 752, 92
Akahori, T., & Ryu, D., 2010, ApJ, 723, 476
Akahori, T., & Ryu, D., 2011, ApJ, 738,134
Akahori, T., Ryu, D., Kim, J., Gaensler, B.M., 2013, ApJ, 767,150
Anderson, J., Beck, R., Bell, M., et al., 2012, Proceedings of "Magnetic Fields in the Universe: From Laboratory and Stars to Primordial Structures", 2011 Aug. 21-27 in Zakopane/Poland, arXiv:1203.2467
Asada, K., Inoue, M., Kameno, S., Nagai, H., 2008, ApJ, 675, 79
Asai, N., Fukuda, N., Matsumoto, R. 2005, Adv. in Space Res. 36, 636
Ascasibar, Y., & Markevitch, M., 2006, ApJ, 650, 102
Arshakian, T.G., Beck, R., Krause, M., Sokoloff, D., 2009, A&A, 494, 21
Arshakian, T.G., & Beck, R., 2011, MNRAS, 418, 2336
Beck, A.M., Dolag, K., Lesch, H., & Kronberg, P.P., 2013, MNRAS (in press), arXiv:1308.3440
Beck, R., & Gaensler, B. M. 2004, New Astronomy Review, 48, 1289
Beck, R., Anderson, J., Heald, G., et al., 2013, Astronomische Nachrichten, 334, 548
Beck, R., & Wielebinski, R., 2013, Planets, Stars and Stellar Systems. Volume 5: Galactic Structure and Stellar Populations, 641
Bernardi, G., Greenhill, L.J., Mitchell, D.A., et al., 2013, ApJ, 771, 105
Bernet, M.L., Miniati, F., Lilly, S.J., 2012, ApJ, 761, 144
Bernet, M.L., Miniati, F., Lilly, S.J., 2013, ApJ, 772, L28
Blasi, P., & Colafrancesco, S., 1999, Astroparticle Physics, 12, 169
Bogdanović, T., Reynolds, C.S., Massey, R., 2011, ApJ, 731, 7
Bonafede, A., Feretti, L, Giovannini, G., et al., 2009a, A&A, 503, 707

Bonafede, A., Giovannini, G., Feretti, L., Govoni, F., & Murgia, M., 2009b, A&A, 494, 429
Bonafede, A., Feretti, L., Murgia, M., et al., 2010, A&A, 513, A30
Bonvin, C., Caprini, C., Durrer, R., 2012, PhRvD 86, 023519
Brentjens, M.A., de Bruyn, A.G., 2005, A&A, 441, 1217
Brentjens, M.A., 2008, A&A, 489, 69
Brentjens, M.A., 2011, A&A, 526, A9
Braun, R, SKA-TEL-SKO-DD-XXX, 2013, SKA1 IMAGING SCIENCE PERFORMANCE
Brown, J.C., 2010, Astronomical Society of the Pacific Conference Series, 438, 216
Brown, S., Farnsworth, D., & Rudnick, L. 2010, MNRAS, 402, 2
Brown, S., & Rudnick, L., 2011, MNRAS, 412, 2
Brunetti, G., 2011, Journal of Astrophysics and Astronomy, 32, 437
Burn, B.J., 1966, MNRAS, 133, 67
Carozzi, T.D., Woan, G., Maaskant, R., 2009, Proceedings of Wide Field Astronomy & Technology for the Square Kilometre Array, Chateau de Limelette, Belgium
Clarke, T.E., & Ensslin, T.A., 2006, AJ, 131, 2900
Condon, J.J., 1984, ApJ, 287, 461
Condon, J.J., Cotton, W.D., Greisen, E.W., et al., 1998, AJ, 115, 1693
Condon, J.J., Cotton, W.D., Fomalont, E.B., et al., 2012, ApJ, 758, 23
Das, S., Kang, H., Ryu, D., Cho, J. 2008, ApJ, 682, 29
Dewdney P.E. et al., 2013, SKA1 system baseline design, SKA report SKA-TEL-SKO-DD-001
Dolag, K., Schindler, S., Govoni, F., Feretti, L., 2001, A&A, 378, 777
Donnert, J., Dolag, K., Lesch, H., Müller, E., 2009, MNRAS, 392, 1008
Dubois & Tessier 2008, A&A, 482, L13
Eilek, J.A., & Owen, F.N., 2002, ApJ, 567, 202
Enßlin, T.A., Biermann, P.L., Klein, U., & Kohle, S., 1998, A&A, 332, 395
Enßlin, T.A., & Gopal-Krishna 2001, A&A, 366, 26
Enßlin, T.A., & Brüggen, M., 2002, MNRAS, 331, 1011
Enßlin T.A., & Vogt C., 2003, A&A, 401, 835
Enßlin, T.A., Pfrommer, C., Miniati, F., & Subramanian, K., 2011, A&A, 527, A99
Feretti, L., Giovannini, G., Govoni, F., & Murgia, M., 2012, A&A Rev., 20, 54
Ferrari, C., Govoni, F., Schindler, S., Bykov, A.M., Rephaeli, Y., 2008, Space Science Reviews, 134, 93
Ferrière, K., & Schmitt, D., 2000, A&A, 358, 125
Ferrière, K. 2007, EAS Publications Series, 23, 3
Fletcher, A., Beck, R., Shukurov, A., et al., 2011, MNRAS, 412, 2396
Farnsworth, D., Rudnick, L., & Brown, S. 2011, AJ, 141, 28
Fujita, Y., Kohri, K., Yamazaki, R., & Kino, M., 2007, ApJ, 663, L61
Fujita Y., & Ohira Y., 2012, ApJ, 746, 53
Fujita Y., & Ohira Y., 2013, MNRAS, 428, 599
Gaensler, B.M., Beck, R., Feretti, L., 2004, New Astronomy Reviews, 48, 1003
Gaensler, B.M., Landecker, T.L., Taylor, A.R., & POSSUM Collaboration, 2010, Bulletin of the American Astronomical Society, 42, #470.13
Gitti, M., Brunetti, G., Setti, G., 2002, A&A, 386, 456
Gießübel, R., Heald, G., Beck, R., Arshakian, T., 2013, arXiv:1309.2539
Gómez, J.L., Roca-Sogorb, M., Agudo, I., et al., 2011, ApJ, 733, 11
Govoni, F., Murgia, M., Feretti, L., et al., 2005, A&A, 430, L5
Govoni, F., Murgia, M., Feretti, L., et al., 2006, A&A, 460, 425
Govoni, F., Dolag, K., Murgia, M., et al., 2010, A&A, 522, 105 Govoni, F., Murgia, M., Xu, H., et al., 2013, A&A, 554, A102
Gressel, O., Elstner, D., Ziegler, U., Ruumldiger, G., 2008, A&A, 486, L35
Guidetti, D., Murgia, M., Govoni, F., et al., 2008, A&A, 483, 699
Guidetti, D., Laing, R.A., Murgia, M., et al., 2010, A&A, 514, A50
Hada, K., Doi, A., Kino, M., et al. 2011, Nature, 477, 185
Hanasz, M., Wóltański, D., Kowalik, K., 2009, ApJ, 706, L155
Heald, G.H, 2009, Cosmic Magnetic Fields: From Planets, to Stars and Galaxies, Proceedings of the Inter-

national Astronomical Union, IAU Symposium, Volume 259, p. 591-602
Heald, G.H., de Bruyn, G., Nijboer, R., et al., 2012, American Astronomical Society Meeting Abstracts, 219, 214.02
Heiles, C., & Haverkorn, M. 2012, Space Science Reviews, 166, 293
Hoeft, M., & Brüggen, M., 2007, MNRAS, 375, 77
Iacobelli, M., Haverkorn, M., Katgert, P., 2013, A&A, 549, A56
Iapichino, L., & Brüggen, M., 2012, MNRAS, 423, 2781
Ideguchi, S., Takahashi, K., Akahori, T., Kumazaki, K. & Ryu, D., PASJ accepted
Johnston-Hollitt, M., 2003, Ph.D. Thesis, University of Adelaide
Kang, H., Ryu, D., & Jones, T.W., 2012, ApJ, 756, 97
Keshet, U., & Loeb, A., 2010, ApJ, 722, 737
Kuchar, P., & Enßlin, T.A., 2011, A&A, 529, A13
Krause, M., Alexander, P., Bolton, R., et al., 2009, MNRAS, 400, 646
Kolatt, T. 1998, ApJ, 495, 564
Laing, R.A., Bridle, A.H., Parma, P., Murgia, M., 2008, MNRAS, 391, 521
Leahy, J.P., 1987, MNRAS, 226, 433
Lobanov, A.P., 1998, A&A, 330, 79
Machida, M., Nakamura, K., Kudo, T., et al., 2013, ApJ, 764, 81
Macquart, J.-P., Ekers, R.D., Feain, I., Johnston-Hollitt, M., 2012, ApJ, 750, 139
Mao, S.A., Gaensler, B.M., Haverkorn, M., et al., 2010, ApJ, 714, 1170
Markevitch, M., 2010, arXiv:1010.3660
Mazzotta, P., & Giacintucci, S., 2008, ApJ, 675, L9
Moss, D., & Sokoloff, D., 2008, A&A, 487, 197
Moss, D., Sokoloff, D., Beck, R., Krause, M., 2010, A&A, 512, A61
Moss, D., Stepanov, R., Arshakian, T.G., et al., 2012, A&A, 537, A68
Moss, D., Beck, R., Sokoloff, D., et al., 2013, A&A, 556, A147
Murgia M., Govoni F., Feretti L., et al., 2004, A&A, 424, 429
Nishikori, H., Machida, M., Matsumoto 2006, ApJ, 641, 862
Oppermann, N., Junklewitz, H., Robbers, G., et al., 2012, A&A, 542, A93
O'Sullivan, S.P., Brown, S., Robishaw, T., et al., 2012, MNRAS, 421, 3300
O'Sullivan, S.P., McClure-Griffiths, N.M., Feain, I.J., et al., 2013a, MNRAS, 435, 311
O'Sullivan, S.P., Feain, I.J., McClure-Griffiths, N.M., et al., 2013b, ApJ, 764, 162
Pentericci, L, Van Reeven, W., Carilli, C.L, Röttgering, H.J.A., Miley, G.K., 2000, A&AS 145, 121
Petrosian, V., 2001, ApJ, 557, 560
Pfrommer, C., & Enßlin, T. A., 2004a, MNRAS, 352, 76
Pfrommer, C., & Enßlin, T. A., 2004b, A&A, 413, 17
Pizzo, R.F., de Bruyn, A.G., Bernardi, G., Brentjens, M.A., 2011, A&A, 525, A104
Planck Collaboration, 2013, A&A 554, 140
Pratley, L., Johnston-Hollitt, M., Dehghan, S., Sun, M., 2013, MNRAS, 432, 243
Radhakrishnan, V., & Rankin, J.M., 1990, ApJ, 352, 258
Ryu, D., Kang, H., Cho, J., & Das, S. 2008, Science, 320, 909
Ryu, D., et al. 2012, Space Science Review, 166, 1
Roediger, E., Brüggen, M., Simionescu, A., et al., 2011, MNRAS, 413, 2057
Roettiger, K., Burns, J. O., Stone, J. M., 1999, ApJ, 518, 603
Rudnick, L., & Blundell, K. M., 2003, ApJ, 588, 143
Rudnick, L., 2011, Journal of Astrophysics and Astronomy, 32, 549
Schleicher, D.R.G., & Beck, R. 2013, A&A, 556, A142
Schnitzeler, D.H.F.M., Katgert, P., de Bruyn, A.G., 2009, A&A, 494, 611
Schnitzeler, D.H.F.M., 2010, MNRAS, 409, L99
Shannon, R.M., & Johnston, S., 2013, MNRAS, 435, L29
Sofue, Y., Machida, M., Kudo, T. 2010, PASJ, 62, 1191
Stasyszyn, F., Nuza, S. E., Dolag, K., Beck, R., & Donnert, J. 2010, MNRAS, 408, 684
Stepanov, R., Arshakian, T.G., Beck, R., Frick, P., & Krause, M., 2008, A&A, 480, 45
Stil, J.M., Krause, M., Beck, R., Taylor, A.R., 2009, ApJ, 693, 1392

Stil, J.M., Taylor, A.R., Sunstrum, C., 2011, ApJ, 726, 4
Takahashi, K., Inoue, S., Ichiki, K., & Nakamura, T., 2011 MNRAS, 410, 2741
Takahashi, K., Mori, M., Ichiki, K., & Inoue, S. 2012, ApJ, 744, L7
Takami, H., Nishimichi, T., Yahata, K., & Sato, K. 2009, JCAP, 6, 31
Takizawa, M. 2008, ApJ, 687, 951
Taylor G.B., Fabian, A.C., Gentile, G., et al., 2007, MNRAS, 382, 67
Taylor, A.R., Stil, J.M., Grant, J.K., et al., 2007, ApJ, 666, 201
Taylor, A.R., Stil, J.M., Sunstrum, C., 2009, ApJ, 702, 1230
Taylor, A.R., & Salter, C.J., 2010, Astronomical Society of the Pacific Conference Series, 438, 402
Tribble, P.C., 1991, MNRAS, 250, 726
Vacca, V., Murgia, M., Govoni, F., et al., 2010, A&A, 514, A71
Vacca, V., Murgia, M., Govoni, F., et al., 2012, A&A 540, 38
van Weeren, R.J., Röttgering, H.J.A., Brüggen, M., & Hoeft, M., 2010, Science, 330, 347
van Weeren, R. J., Röttgering, H. J. A., Rafferty, D. A., et al., 2012a, A&A, 543, A43
van Weeren, R. J., Röttgering, H. J. A., Intema, H. T., et al., 2012b, A&A, 546, A124
Vollmer, B., Soida, M., Beck, R., et al. 2007, A&A, 464, L37
Xu, Y., Kronberg, P. P., Habib, S., & Dufton, Q. W. 2006, ApJ, 637, 19
Xu, H., Li, H., Collins, D. C., Li, S., & Norman M. L. 2009, ApJL, 698, L14
Xu, H., Govoni, F., Murgia, M., et al., 2012, ApJ, 759, 40
Weiler, K.W., & de Pater, I., 1983, ApJS, 52, 293
Weżgowiec, M., Urbanik, M., Vollmer, B., et al. 2007, A&A, 471, 93
Widraw, L., et al. 2012, Space Science Review, 166, 37
Wolleben, M., Landecker, T.L., Carretti, E., et al. 2009, IAU Symposium, 259, 89
Yamazaki, D. G., Kajino, T., Mathews, G. J., & Ichiki, K. 2012, Physics Reports, 517, 141
Zavala, R.T., & Taylor, G.B., 2004, ApJ, 612, 749
ZuHone, J.A., Markevitch, M., Brunetti, G., & Giacintucci, S. 2013, ApJ, 762, 78